A Shoulder Mechanism for Assisting Upper Arm Function with Distally Located Actuators

Michael Jones, Connor Bouffard, and Babak Hejrati*, *Member, IEEE*

Abstract— **This paper presents a new design for a shoulder assistive device based on a modified double parallelogram linkage (DPL). The DPL allows for active support of the arm motion in the sagittal plane, while enabling the use of a distally located motor that can be mounted around the user's waist to improve the weight distribution. The development of the DPL provides an unobtrusive mechanism for assisting the movement of the shoulder joint with a wide range of motion. This design contains three degrees-of-freedom (DOFs) and a rigid structure for supporting the arm. The modified DPL uses a cable-driven system to transfer the torque of the motor mounted on the user's back through the links to the arm. The proposed design assists with the flexion/extension of the arm, while allowing the adduction/abduction and internal/external rotations to be unconstrained. A kinematic analysis of the cable system and linkage interaction is presented, and a prototype is fabricated to verify the proposed concept.**

I. Introduction

Robotic exoskeletons can be used to assist people with limited range of motion in performing daily tasks. Upper-limb exoskeletons are particularly useful for their assistance with daily activities such as eating, lifting objects, brushing teeth etc. More recently, the importance of arm swing for gait rehabilitation has been presented by Hejrati et al. [1], [2], which capitalizes on the design of a wearable assistive device to induce arm swing. The challenge with designing an exoskeleton for the arm is to determine the sufficient number of degrees of freedom (DOFs) to provide adequate assistance while keeping the weight of the mechanism low to avoid user fatigue.

Several designs exist for overcoming this problem such as a soft cable-driven exoskeleton, which relies on the user's own body to provide the structure. A soft exoskeleton has the benefit of moving the joint without causing joint misalignment because the cables use the skeletal structure of the body for support [3], [4]. Dinh et al. [4] attempted to mitigate slacking and backlashing of the cable-driven systems by pre-tensioning the cables and using a nonlinear adaptive controller to actuate the system. Barns et al. [2] proposed a design which uses a pulley-belt mechanism and a cable-driven haptic paddle to transfer the torque generated by the distal motors located around the user's waist to their arms.

A spherical mechanism provides a rigid structure that closely follows the shoulder's movement and can fully support the movement of the arm [5], [6]. Hsieh et al. [6] used linear stepper motors instead of DC motors. This actuator change allowed them to use two slider-crank mechanisms and two spherical mechanisms to design a shoulder joint with 2 active and 4 passive DOFs. Although this design was unobtrusive, compact, and lightweight, the spherical mechanism is a complex solution and requires many components to follow the shoulder movements.

A design by Liu et al. [7] can provide assistance up to 30% of a human's arm weight during flexion/extension. The design has one powered and two passive DOFs, therefore it is relatively light and only weighs 5.1 kg. A similar mechanism by Sui et al. [8] provides 4 active and 1 passive DOFs and weighs 8.4 kg for both arms. These designs focus on reducing the weight of the mechanism, but only provide a fraction of the lifting force that a healthy person could exert. A design by Ebrahimi et al. [9] has 3 active and 9 passive DOFs and can generate up to 40 N-m of torque for shoulder flexion/extension and up to 24 N-m of torque for elbow flexion/extension. A tradeoff between these design concepts would be necessary to satisfy both capability and weight requirements.

This paper presents a modification to the double parallelogram linkage (DPL), which is used in previous studies [10], [11] to allow unconstrained internal/external rotations, and use cables to transfer the torque through a rigid mechanism. The proposed mechanism uses a DPL to provide 3 DOFs on the shoulder: 1 active DOF for assisting arm flexion/extension and 2 passive DOFs for other rotations. The system is intended to be used as an assistive mechanism to augment the user's arm strength during lifting tasks. Therefore, its generated torque will be low to keep the weight down. The conceptual design, geometric analysis, and prototyping of the mechanism are presented in this paper.

II. Exoskeleton Conceptual Design

The design of the shoulder mechanism uses a combination of a DPL and a modified cable drive. The DPL shown in Fig. 1 allows for internal/external rotation (left arm in Fig. 1 (a)) by aligning the output link with the outside of the arm. The input shaft mounts on the torso and aligns with the axis of abduction/adduction rotation of the shoulder and provides a passive DOF. The output shaft aligns with the axis of flexion/extension rotation and provides the active DOF. The sizing of the mechanism to the user is determined by D_1 and D_2 and can be adjusted to fit a wider variety of sizes.

By combining the DPL with the modified pulley mechanism, the torque from the input shaft mounted onto the torso can be transferred to the output shaft connected to the

*The authors are with the Department of Mechanical Engineering, University of Maine, ME 04669 USA. (Corresponding author e-mail: babak.hejrati@maine.edu)

978-1-5386-1311-5/19/$31.00 ©2019 IEEE

user's arm. The input axis is along the vertical axis while the output axis is horizontal. In this configuration, the cable is twisted 90° as it goes from the input to the output.

The power for the mechanism comes from a distally located stepper motor that uses a cable-driven system to transfer the torque to the output shaft. As shown in Fig. 1, two cables transfer the torque from the motor to the input shaft at point A and from the input shaft to the output shaft at point C. The input shaft is mounted on the user's back perpendicular to the transverse plane. The input shaft is the interaction point between the two cables used in the system: the motor cable and the DPL cable. The torque is transferred from the input shaft to the output shaft similar to a simple cable drive mechanism with two pulleys as seen in Fig. 2. This diagram simplifies the mechanism and allows for analysis of the power transfer. Point B is a passive DOF hinge joint allowing link 1 and link 2 to actuate freely based on the user's motion. Point C corresponds to the powered flexion/extension motion in the arm. The pulleys are connected with a continuous cable loop. It is desired for B to be a free center-of-rotation while A powers the rotation of C. The issues with a simple pulley layout are that cable tensioning and slacking occur during the motion. Cable slacking and cable tensioning happen simultaneously when the mechanism actuates at B to allow for internal/external rotation. For the purposes of examining them, the cable tensioning and slacking are explained separately.

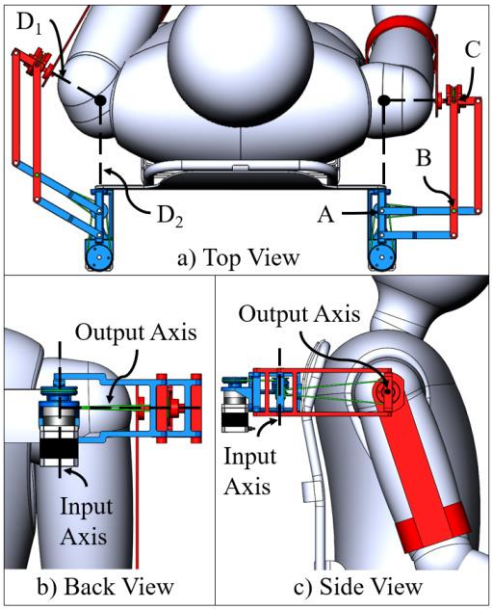

Fig. 1: Three-views of the double parallelogram mechanism on the shoulder, (a) top view with the left arm at an angle, (b) back view and, (c) side view.

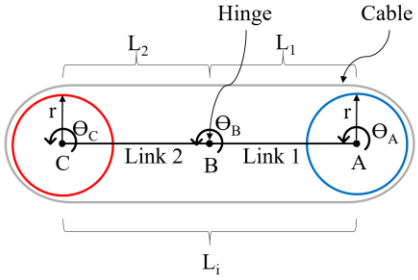

Fig. 2: Cable and pulley mechanism schematics.

A. Cable Tensioning

Cable tensioning occurs when the motor initially starts to rotate the input pulley, or the mechanism is actuated at B. Fig. 3 shows a scenario where A is rotated by the motor, B is free to rotate, and C is locked. This case simulates the scenario that the user wants assistance from the motor to raise their arm in flexion direction without moving their arm in internal/external rotation. Point C is locked because during the motion the output pulley, which is connected to the user's arm, experiences significant resistance. When the pulley at A is rotated counter-clockwise, tension is created in the cable on the bottom. Since point B is the only place with free rotation, this tension will result in an upwards movement of point B as shown in Fig. 4. The movement and subsequent rotation of point B is an undesired outcome of the motor actuation.

B. Cable Slacking

Due to the tensioning of the cable, the opposite side of the cable becomes slack as soon as tensioning occurs. Fig. 4 shows the result of the motor rotation. The final distance L_f between the pulleys in Fig. 4 is shorter than the initial distance L_i between the pulleys in Fig. 3. Since the distance between the pulleys decreases, the cable will not stay in contact with the pulleys and will no longer stay tensioned.

The same pulley setup can be kept, and a modification is made by constraining the cable at B so that the cable passes through the axis of rotation at B. This modification can be seen in Fig. 5. The cable is constrained at B by using a low friction guide hole to prevent the cables from escaping. By passing the cables over the axis of B, the tension will be maintained in the cable and slack will not be created. No torque will be generated around point B from the tension force in the cable because the moment arm of the cable is reduced to zero about B. The input pulley can still transfer torque to the output pulley similar to the simple pulley configuration because the pulleys are connected by a continuous loop of cable.

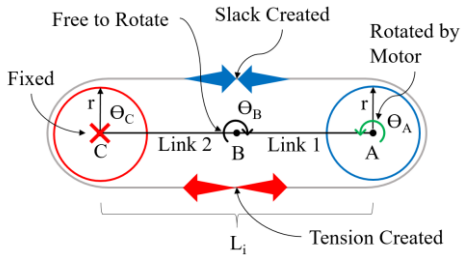

Fig. 3: Tension created when the motor rotates the input pulley.

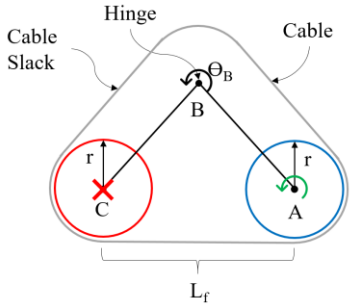

Fig. 4: Slack created when the pulley at point B rotates.

This modification separates and isolates the torque transfer from A to C from the rotation at B. When the user wants to rotate their arm across their body in internal/external rotation, θ_B changes but the cable only bends at point B and does not create tension or slack as shown in Fig. 6.

The total length of the cable on each side of point B is constant and can be seen by comparing Fig. 5 with Fig. 6. At an angle of $\theta_B = \pi$ shown in Fig. 5, the total length of the cable on the right-hand side (RHS) of B noted by m is given by:

$$m = C_1 + C_2 + C_3 \quad (1)$$

At some other arbitrary angles of θ_B shown in Fig. 6, the total length of cable on the RHS of B noted by n is given by:

$$n = C_4 + C_5 + C_6 \quad (2)$$

The values for m and n can be found by calculating the total length of the cable using the triangles shown in Fig. 7, where $x = \sqrt{{L_1}^2 - r^2}$, $y = rsin(\theta)$, and $\sin(\theta) = r/L_1$. These relations are based on a small angle approximation for θ to assume y is a straight line. Also, $C_1 = C_4 = \pi * r$.

$$m = n = 2 * (\sqrt{L_1^2 - r^2} + \frac{r^2}{L_1}) + \pi * r \quad (3)$$

By constraining the cable in at the point of rotation where no torque is desired, the tension of the cable will be isolated from the rotation of point B. The same analysis as in (1)-(3) can be done to find the length of cable on the left-hand side (LHS) of B. For any angle θ_B, the total length of the cable (both on the LHS and RHS of B) remains constant, therefore no tension is created.

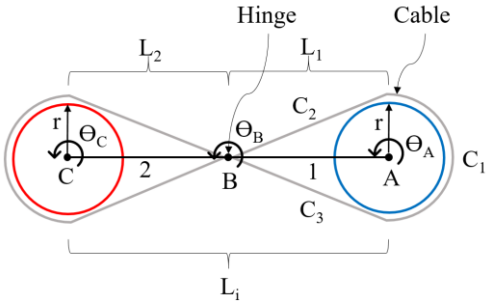

Fig. 5: Modified cable and pulley mechanism with cable constrained at B.

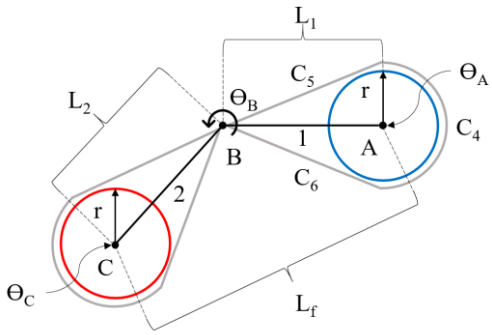

Fig. 6: Cable is kept in tension when the modified pulley system bends at B.

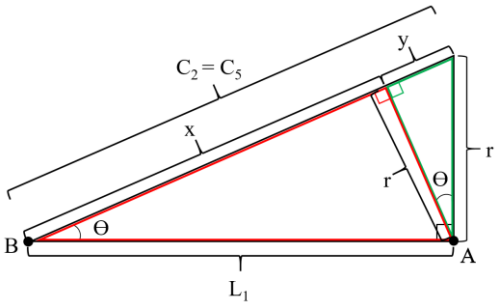

Fig. 7: Geometric diagram to find the cable length on the RHS of B.

III. Construction of the Mechanism

The prototype of the shoulder mechanism is made using an additive manufacturing process. The DPL links can be sized to fit the dimensions of the user's body. The DPL mounts to the user on a backpack in the transverse plane as shown in Fig. 1. The output shaft is normal to the user's arm as shown in Fig. 1. As the cable goes from the input to the output shaft, it twists 90° to account for the shafts being oriented in different directions. The DPL actuation can be seen in Fig. 8, where the output shaft with a red marker rotates around a remote center. The cable follows the path of the links so that it does not interfere with the user.

IV. Experiments and Results

An experiment is performed on the power transmission system of the mechanism to measure the rotation between the input and output shafts. A motor is connected to the input shaft to provide power to the mechanism. Measurements are made with a potentiometer on the input and output shafts to plot the rotation of the input and output. A 360-degree freely rotating potentiometer is used for the input shaft because it is expected that this shaft will rotate more than 360 degrees. A 300-degree potentiometer is used for the output shaft because the output shaft does not rotate a full revolution given that it is connected to the arm. The output shaft can rotate the arm for an approximate range of 200 degrees in the flexion/extension direction, but this range can be limited if less movement is desired. By using the motor to rotate the input shaft, the cable will rotate the output shaft and the potentiometers will measure the exact rotation of each shaft. The diameters of the input and output pulleys predict the slope of the theoretical linear relationship between the input and output angles. It is expected that the experimental results will deviate from this theoretical line due to the imperfections in the constructed mechanism.

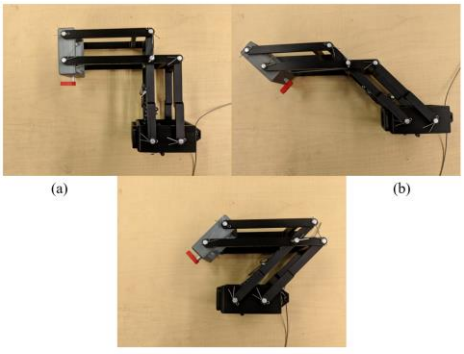

Fig. 8: Actuation of DPL in throughout the internal/external rotation, (a) 90° position, (b) open position, (c) closed position.

The experiments are performed for three different positions of the DPL: (1) the links are at a 90-degree angle as shown in Fig. 8 (a), (2) the DPL is fully open as shown in Fig. 8 (b), and (3) the DPL is fully closed as shown in Fig. 8 (c). The test results are shown in Figs. 9-11.

Figs. 9 and 10 show the responses of the system in the 90-degree and fully open positions. The experimental responses are slightly below the ideal response which means that there was a lag between the input and output shaft rotations. The average slope of the responses is slightly lower than the expected line. These discrepancies are due to imperfections with the cable tensioning and tolerances in the mechanism. The deviations from the ideal line and the experimental results in Figs. 9 and 10 are mainly due to the lack of an appropriate pre-tensioning of the cable that actuates the output shaft by the input shaft. Fig. 11 shows the response curve when the mechanism is at the fully closed position. The response follows the expected path much closer. A reason for this curve being closer to the ideal response is because when the cable is bent at a sharp angle, the bend radius of the cable causes it to come under a slight tension. However, the excessive pre-tensioning due to this configuration rotates the output shaft without the input having moved (backlash issue), and this causes the difference between the curves in Fig. 11. This tension causes the cable to reduce slack and respond quicker. There is also inaccuracy in the potentiometer at lower voltages and our measurement device. Overall, these experiments demonstrate that the concept of the modified DPL mechanism gives the expected results and is a viable design.

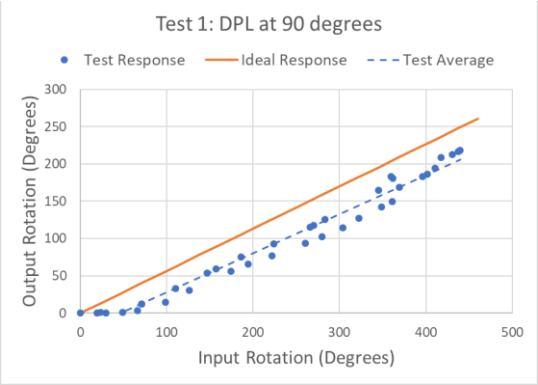

Fig. 9: Test results of pulley action with DPL at 90° position

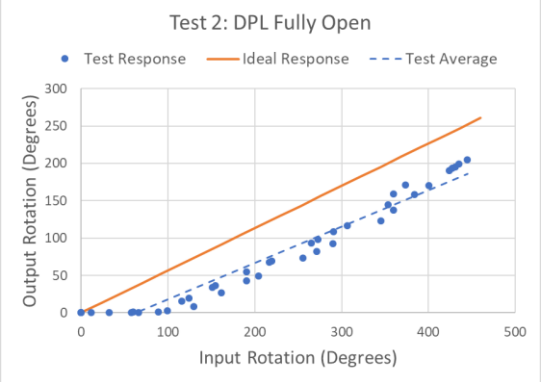

Fig. 10: Test results of pulley action with DPL at open position.

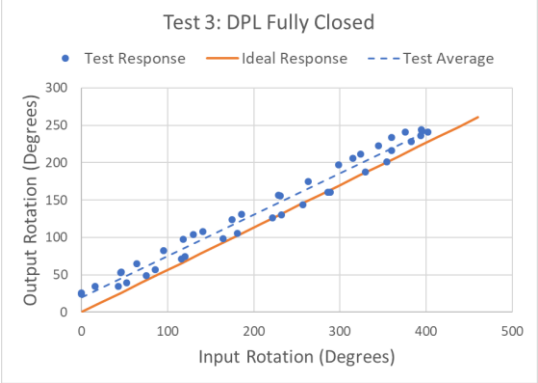

Fig. 11: Test results of pulley action with DPL at closed position.

V. Conclusion and Future Work

This paper focuses on the kinematic design of a novel assistive shoulder exoskeleton that uses a modified cable-driven DPL mechanism to allow for the use of distally located motors. In the current design, the input pulley causes an unintended tensioning when the DPL is moving due to the input axis being perpendicular to the transverse plane. This will be addressed in the future designs by aligning the input pulley axis in-plane with the coronal plane.

References

[1] B. Hejrati, A. Merryweather, and J. J. Abbott, "Generating Arm-swing Trajectories in Real-time Using a Data-driven Model for Gait Rehabilitation with Self-selected Speed," *IEEE Transactions on Neural systems and Rehabilitation Engineering* 26, no. 1 (2018): 115-124.

[2] O. R. Barnes, B. Hejrati, and J. J. Abbott, "An Underactuated Wearable Arm-swing Rehabilitator for Gait Training," *in 2015 IEEE Int. Conf. Robotics and Automation (ICRA)*, pp. 4998-5003. IEEE, 2015.

[3] I. Galiana, F. L. Hammond, R. D. Howe, and M. B. Popovic, "Wearable soft robotic device for post-stroke shoulder rehabilitation: Identifying misalignments," *in 2012 IEEE/RSJ Int. Conf. on Intel. Rob. and Syst.*, pp. 317–322. IEEE, 2012.

[4] B. K. Dinh, M. Xiloyannis, L. Cappello, C. W. Antuvan, S. C. Yen, and L. Masia, "Adaptive backlash compensation in upper limb soft wearable exoskeletons," *Rob. Auton. Syst*., 92 (2017),173–186.

[5] H. S. Lo and S. S. Q. Xie, "Optimization of a redundant 4R robot for a shoulder exoskeleton," in 2013 IEEE/ASME Int. Conf. on Adv. Int. Mechatronics, pp. 798–803. IEEE, 2013.

[6] H. C. Hsieh, D. F. Chen, L. Chien, and C. C. Lan, "Design of a Parallel Actuated Exoskeleton for Adaptive and Safe Robotic Shoulder Rehabilitation," *IEEE/ASME Trans. Mechatronics* 22, no. 5 (2017): 2034–2045.

[7] C. Liu, C. Zhu, H. Liang, M. Yoshioka, Y. Murata, and Y. Yu, "Development of a light wearable exoskeleton for upper extremity augmentation," in *2016 23rd Int. Conf. on Mechatronics and Machine Vision in Practice (M2VIP),* pp. 1–6. IEEE, 2016.

[8] D. Sui, J. Fan, H. Jin, X. Cai, J. Zhao, and Y. Zhu, "Design of a wearable upper-limb exoskeleton for activities assistance of daily living*," in 2017 IEEE Int. Conf. on Adv. Intel. Mechatronics (AIM)*, pp. 845–850. IEEE, 2017.

[9] A. Ebrahimi, "Stuttgart Exo-Jacket: An exoskeleton for industrial upper body applications," *in 2017 10th Int. Conf. on Human Syst. Interactions (HSI)*, pp. 258–263. IEEE, 2017.

[10] S. Bai, S. Christensen, and M. R. U. Islam, "An upper-body exoskeleton with a novel shoulder mechanism for assistive applications," *in 2017 IEEE Int. Conf. on Adv. Intel. Mechatronics (AIM)*, pp. 1041–1046. IEEE, 2017.

[11] S. Christensen and S. Bai, "Kinematic Analysis and Design of a Novel Shoulder Exoskeleton Using a Double Parallelogram Linkage," *J. Mech. Robot.*10, no. 4 (2018): 41008.